J Mater Sci (2007) 42:2383–2386
DOI 10.1007/s10853-006-1300-4

Effect of composition on the crystallization and magnetic properties of Fe–Co–Si–B–Nb amorphous alloys

Hyang-Yeon Kim

Received: 27 April 2005 / Accepted: 23 January 2006 / Published online: 17 December 2006

Abstract The crystallization behavior and magnetic properties of $Fe_{62}Co_{10}Si_{15-x}B_{18-y}Nb_{(x+y)-5}$ amorphous alloys with $x = 0$–5 and $y = 0$–5 were examined. Primary crystallization temperature of $Fe_{62}Co_{10}Si_{15-x}B_{13}Nb_x$ and $Fe_{62}Co_{10}Si_{10}B_{18-y}Nb_y$ alloys increased with the addition of Nb. The primary and secondary crystallization temperatures were well separated when the Nb content is above 4 at%. The alloys with 15–18 at% B showed a distinct supercooled region. The Nb addition decreased the Curie temperature as well as room temperature saturation magnetization. The glassy-type $Fe_{62}Co_{10}Si_{10}B_{18}$ alloy exhibited good soft magnetic properties as well as a supercooled liquid region of 39 K. The finding of the glassy-type Fe-based alloy without Nb element exhibiting high Bs above 1.4 T is promising for future use as a soft magnetic glass material.

Introduction

The microstructure and soft magnetic behavior of nanocrystalline Fe–Cu–Nb–Si–B alloys have been studied extensively for the last 10 years [1–4]. Their excellent soft magnetic characteristics arise from randomly oriented bcc Fe-rich ultrafine grain structure embedded in a residual amorphous matrix [5]. Nb acts as the grain growth inhibitor during crystallization process and the addition of 3–4 at% Nb is necessary for getting the desired grain size for good soft magnetic properties. Critical percentages of Si and B are also required to form an ordered DO_3 structure for the nanocrystalline phase [6]. However, Fe–Cu–Nb–Si–B-based alloys are not suitable for the high temperature applications as they have relatively low Curie temperatures. Recently, much attention has been paid to the development of alloys for high temperature applications [7–9]. Partial substitution of Fe by Co in Fe–Cu–Nb–Si–B alloys is strong candidate for such high temperature applications. However, crystallization process in Fe-based glassy system changes with the addition of Co. It has been reported that the nucleating element Cu is not always needed for nanocrystallization when Co is added in the above alloy systems [10].

Applications of Fe–Co-based soft magnetic materials at high temperature require high saturation induction and high Curie temperature so that the materials could be used at elevated temperatures without major structural degradation that affects the magnetic properties. High saturation induction could be achieved in Fe–Co-based amorphous system by partial crystallization of α-(Fe–Co) phase having high saturation induction and Curie temperature. During this process B-rich secondary phase that deteriorates good soft magnetic nature of the materials should be suppressed. Thus Nb and the metalloids are major factors for successfully implementing Fe–Co–Si–B–Nb glassy alloy for high temperature application.

The aim of the present paper is to examine the influence of Nb and the metalloids (Si and B) on the

H.-Y. Kim
Institute for Materials Research, Tohoku University, Sendai 980-8577, Japan

Present Address:
H.-Y. Kim (✉)
R&D Team, ILJIN Electric Co., Ltd., Seoul 121-040, Korea
e-mail: hyangyeon.kim@iljin.co.kr

crystallization and soft magnetic properties of Fe–Co–Nb–Si–B amorphous alloys. An optimum Nb concentration, which will put primary and secondary crystallization wide apart so that during annealing process the secondary crystallization does not takes place, will also be evaluated in the present work.

Experimental procedure

Ingots with nominal composition of $Fe_{62}Co_{10}Si_{15-x}B_{18-y}Nb_{(x+y)-5}$ with x = 0–5 and y = 0–5 (all in at%) were prepared by arc melting. Rapidly solidified ribbons with 1 mm wide and 0.025 mm thick were produced by ejecting the molten ingot on a Cu-wheel rotating at a circumferential velocity of 40 m/s. The amorphous nature of the ribbons was confirmed by XRD analysis. The crystallization behavior was examined by differential scanning calorimetry (Seiko Instrument Inc., DSC–6300) at a heating rate of 0.67 K/s. The coercivity was evaluated at a quasi dc field using a B-H analyzer (Denshi Jiki Industry Co. Ltd., Mode-BH-5501). The effective permeability (μ_e) was measured using an impedance analyzer (Agilent, 4294A) at a magnetizing field of 0.5 A/m and a frequency 1 kHz. The saturation magnetization was measured using a VSM (Riken Denshi, Model-BHV-55) at a field of 800 kA/m. The annealing was performed in a high vacuum (10^{-5} Torr) state. The crystallized phases were analyzed by X-ray diffractogram (Rigaku, Rint 2200 PC(L)) using Cu target.

Results and discussions

Figures 1 and 2 show DSC curves of the $Fe_{62}Co_{10}Si_{15-x}B_{13}Nb_x$ and $Fe_{62}Co_{10}Si_{10}B_{18-y}Nb_y$ amorphous alloys, respectively. At x = 0 and y = 5, i.e. Nb = 0, B = 13 and Si = 15, one can see the two phases at the first stage crystallization (Fig. 1). To identify these phases, the alloy was annealed at 873 K for 15 min. Two major phases, α-FeCo(Si) and Fe_2B were observed after the first stage of crystallization. There is a drastic change in the crystallization behavior for $Fe_{62}Co_{10}Si_{14}B_{13}Nb_1$ containing 1 at% Nb. A large secondary crystallization peak was observed with an onset of 960 K and a peak temperature 844 K well separated from the primary crystallization in $Fe_{62}Co_{10}Si_{11}B_{13}Nb_4$ containing 4 at% Nb. The onset temperature of the primary crystallization increases with increasing Nb concentration, as shown in Fig. 3a. The secondary crystallization mode also changed with the variation of Si and Nb concentration. At x = 2 and 3, broad exothermic peaks with

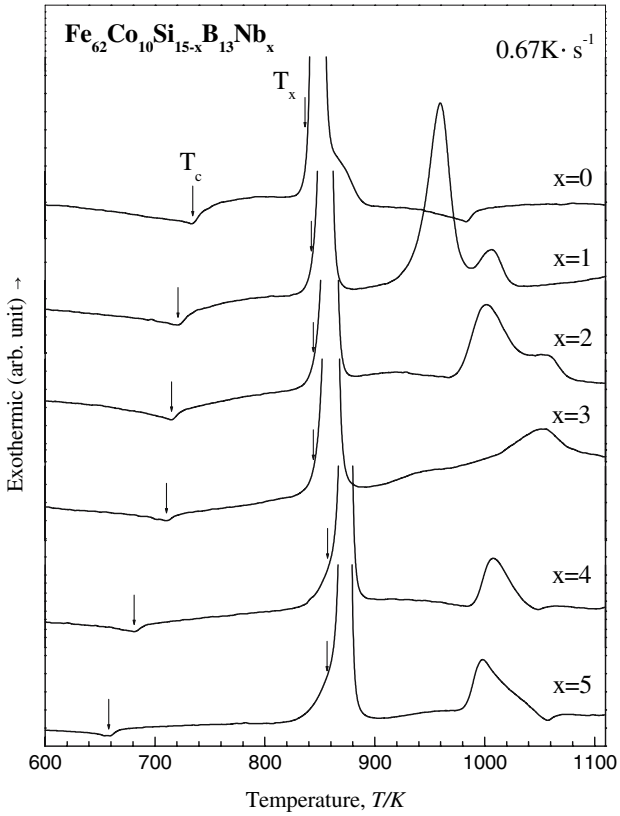

Fig. 1 DSC curves of melt-spun $Fe_{62}Co_{10}Si_{15-x}B_{18-y}Nb_{(x+y)-5}$ alloys with y = 5 and x = 0–4

peak temperatures 916 and 938 K after the primary crystallization were observed. At x = 4, i.e. in $Fe_{62}Co_{10}Si_{11}B_{13}Nb_4$ alloy, two distinct primary peak with an onset temperature of 866 K and onset of secondary crystallization peak of 990 K were observed. Similar behavior was also observed when x = 5 and the onset temperatures was 983 K.

To examine the influence of Nb and B on the properties of the $Fe_{62}Co_{10}Si_{15-x}B_{18-y}Nb_{(x+y)-5}$ alloys, Si was fixed to be 10% (Fig. 2). These alloys showed a supercooled liquid region in the range of y = 0–3. The largest supercooled region was obtained for the $Fe_{62}Co_{10}Si_{10}B_{18}$ alloy. No glass transition was observed for the alloy with y = 4 and above. The glass transition temperature(T_g) and the supercooled region ($\Delta T_x = T_x - T_g$) are shown in Fig. 3b, c, respectively. The first-stage crystallization phase are α-FeCo(Si), Fe_2B, Fe_3Si and CoSi. Like in the other alloy systems examined in the present study, the crystallization behavior also changed with the addition of Nb in $Fe_{62}Co_{10}Si_{15-x}B_{18-y}Nb_{(x+y)-5}$. The crystallization temperature increased with Nb concentration. The increase in T_x was less in case of B and Nb variation than that of Si and Nb variation.

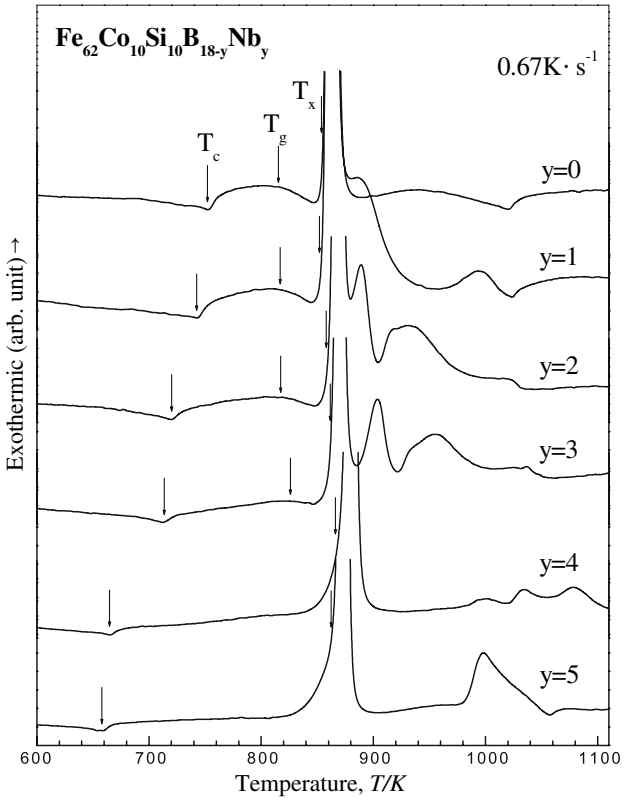

Fig. 2 DSC curves of melt-spun $Fe_{62}Co_{10}Si_{15-x}B_{18-y}Nb_{(x+y)-5}$ alloys with $x = 5$ and $y = 0$–5

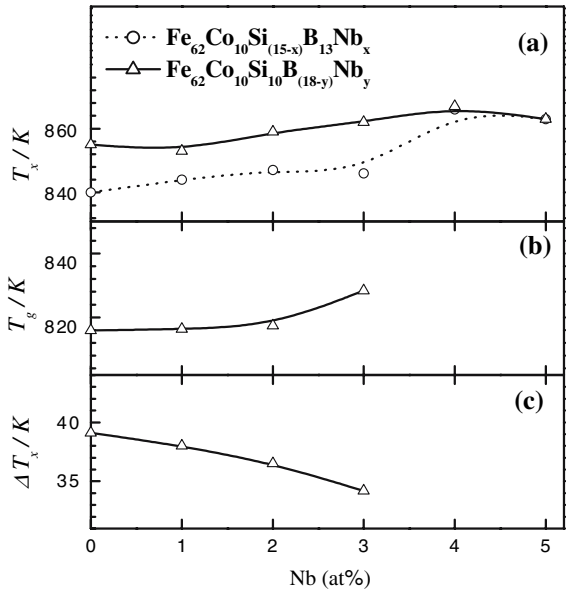

Fig. 3 Changes in (**a**) crystallization temperature, T_x, (**b**) glass transition temperature, T_g and (**c**) supercooled liquid region, ΔT_x with Nb concentration for $Fe_{62}Co_{10}Si_{15-x}B_{13}Nb_x$ (○) and $Fe_{62}Co_{10}Si_{10}B_{18-y}Nb_y$ (Δ) glassy alloys

Figure 4 shows the influence of Si, B and Nb on the intrinsic magnetic properties like Curie temperature measured from the DSC curve and the saturation

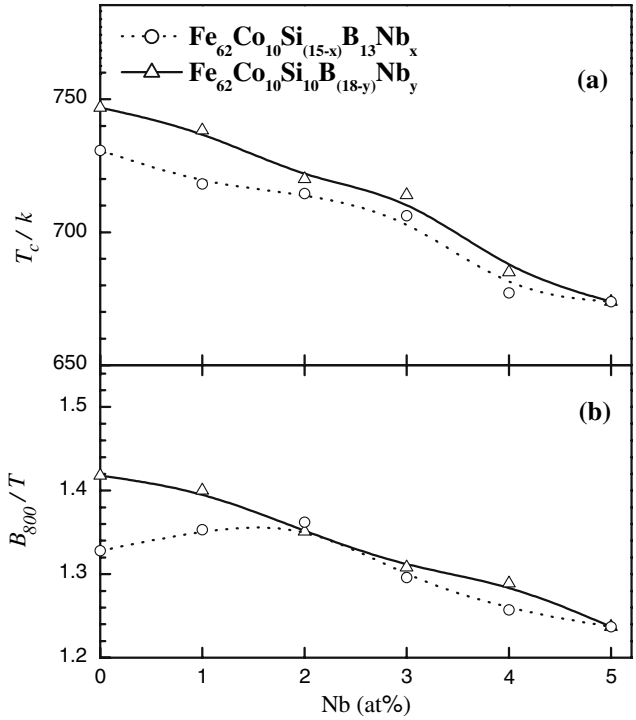

Fig. 4 Changes in (**a**) Curie temperature, T_c and (**b**) room temperature saturation magnetization, B_s with Nb concentration for $Fe_{62}Co_{10}Si_{15-x}B_{13}Nb_x$ (○) and $Fe_{62}Co_{10}Si_{10}B_{18-y}Nb_y$ (Δ) glassy alloys

magnetization measured using a VSM. In case of $Fe_{62}Co_{10}Si_{15-x}B_{13}Nb_x$, the Curie temperature (T_c) and the saturation magnetization (B_s) decreased slowly from 731 K and 1.33 T, respectively, for Nb = 0 (Fig. 4a, b). However, significant reduction of T_c to 677 K and B_s to 1.26 T was observed when $x = 4$ in $Fe_{62}Co_{10}Si_{15-x}B_{13}Nb_x$ alloy. To examine the influence of B and Nb on the intrinsic properties, T_c and B_s were measured for the melt-spun $Fe_{62}Co_{10}Si_{10}B_{18-y}Nb_y$ alloys. At $y = 0$, both T_c (=747 K) and B_s (=1.42 T) were higher as compared to these of $Fe_{62}Co_{10}Si_{15}B_{13}$ alloy. This behavior continued up to $y = 4$ where significant reductions in both the intrinsic properties were observed.

Figure 5 shows soft magnetic properties of coercivity and effective permeability for the $Fe_{62}Co_{10}Si_{15-x}B_{18-y}Nb_{(x+y)-5}$ alloys. The coercivity (Fig. 5a) decreases from 11.9 A/m to 3.4 A/m by the addition of 4 at% Nb leading to the partial replacement of Si in $Fe_{62}Co_{10}Si_{15}B_{13}$ alloy. The effective permeability of the $Fe_{62}Co_{10}Si_{15-x}B_{13}Nb_x$ alloy increased substantially (Fig. 5b) by the addition of 4 at% Nb from 1.37×10^3 for $x = 0$ to about 3.64×10^3 for $x = 4$. Although coercivity increases by the addition of more Nb content for $Fe_{62}Co_{10}Si_{10}B_{13}Nb_5$ alloy, an increasing trend in the effective permeability with Nb addition is recognized. Superior soft magnetic characteristics, i.e. low

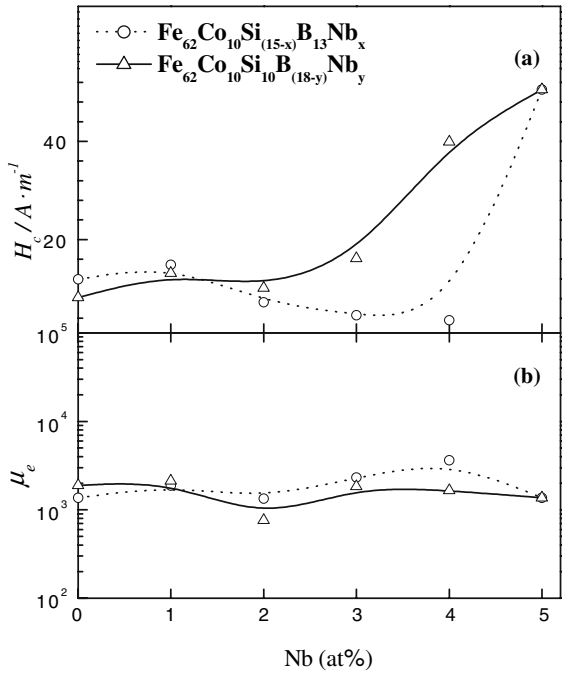

Fig. 5 Changes in (**a**) coercivity, H_c (**b**) permeability, μ_e at 1 kHz under 0.5 A/m, with Nb concentration for $Fe_{62}Co_{10}Si_{15-x}B_{13}Nb_x$ (○) and $Fe_{62}Co_{10}Si_{10}B_{18-y}Nb_y$ (Δ) glassy alloys

coercivity and high permeability, was also obtained for $Fe_{62}Co_{10}Si_{11}B_{13}Nb_4$ alloy. The coercivity increased and effective permeability decreased by the addition of more Nb for the alloy series of $Fe_{62}Co_{10}Si_{10}B_{18-y}Nb_y$. These results indicate that soft magnetic properties by the addition of Nb of Fe–Co–Si–B system are enhanced, though the saturation magnetization and Curie temperature decrease.

Conclusions

We examined thermal stability and magnetic properties of melt-spun $Fe_{62}Co_{10}Si_{15-x}B_{18-y}Nb_{(x+y)-5}$ amorphous ribbons with the variation of x and y from 0 to 5. The alloys containing more than 4 at% Nb showed a wide temperature interval between primary and secondary crystallization phases. Such alloys should be useful for enhancing soft magnetic properties by partial crystallization of α-FeCo(Si) primary phase. The alloys with 4% Nb has excellent soft magnetic properties with lower coercivities below 3.5 A/m and high effective permeability of about 3.64×10^3 in the as-melt spun state. Although the coercivity increases when the Nb content is 4 at% and above, the present soft magnetic properties and wide temperature interval between primary and secondary crystallization peaks suggest that $Fe_{62}Co_{10}Si_{15-x}B_{18-y}Nb_{(x+y)-5}$ glassy alloys with x and y close to 4 would have been a good candidate among the Fe–Co-based glassy alloys for high temperature soft magnetic applications.

References

1. Yoshizawa Y, Oguma S, Yamauchi K (1988) J Appl Phys 64:6044
2. Makino A, Bitoh T, Inoue A, Masumoto T (1997) J Appl Phys 81:2736
3. Suzuki K, Makino A, Inoue A, Masumoto T (1991) Jpn J Appl Phys 30:1729
4. Panda AK, Chattoraj I, Mitra A (2000) J Magn Magn Mater 222:263
5. Herzer G (1990) IEEE Trans Magn 25:3327
6. Muller M, Mattern N, Illgen L (1991) Z Metallkde 82:895
7. Shen B, Kimura H, Inoue A (2002) Mater Trans 43:589
8. Zhang W, Inoue A (2001) Mater Trans 42:1142
9. Willard MA, Laughlin DE, McHenry ME, Thoma D, Sickafus K, Cross JO, Harris VG (1998) J Appl Phys 84:6773
10. Ping DH, Wu YQ, Hono K, Willard MA, McHenry ME, Laughlin DE (2001) Scripta Mater 45:781